State of Stress of Subducting Slabs from Viscoelastic Plane Strain Numerical Modelling

Eugenio Carminati[1*], Patrizio Petricca[1]
[1]Dipartimento di Scienze della Terra, SAPIENZA Università di Roma, Roma, Italy
*eugenio.carminati@uniroma1.it

Abstract: Using 2D viscoelastic plane strain models we investigate the dependency of the stress field of slabs on geometry and kinematics of subduction zones (relative velocity of interacting plates and their absolute velocity with respect to the mantle). We conclude that the concentration of Von Mises stress is controlled by the geometry (curvature) of the slab and that downdip compression in subducting slabs is enhanced by mantle flow opposing the dip of the slab, whereas overall downdip extension is favoured by mantle flow in the same direction of the slab dip.

Keywords: viscoelastic, plane strain, 2D, subduction zones, state of stress.

1. Introduction

The Earth's outer shell (named lithosphere) is divided into plates that move relatively and with respect to the deeper shell (named mantle). The convergence between two plates is normally accommodated by underthrusting of one plate (named slab) under the other. This process is termed subduction and controls a large part of volcanism and seismicity worldwide. Slabs worldwide show a large variability regarding their state of stress. Some are characterised by downdip compression and others by extension.

The downwelling of the plate is accompanied by thermal and metamorphic processes that may potentially increase the density of the slab. Subducting slabs are thought to be denser than the surrounding mantle and this density contrast could provide a pull from the slab on the entire subducting plate (slab pull process). In principle slab pull should enhance down-dip extension in the slab, which contrasts with the above described variability of the stress fields observed worldwide. The dynamics of subduction zones may also be controlled by the relative motion of the lithosphere with respect to the underlying mantle. In this work we evaluate for the first time the effects of plate kinematics on the state of stress of the subducting lithosphere (in terms of Von Mises stresses and principal stress axes orientations) using COMSOL Structural Mechanics Module.

2. State of stress of subducting slabs

The state of stress within subducting slabs is revealed by seismicity. Shallow seismic events in the trench-outer-rise generally indicate a transition from tension to compression with depth (Seno and Yamanaka, 1996), consistent with bending of the plate prior to subduction. Intermediate seismicity (focal depths between 100 km and 300 km; Isacks and Molnar, 1971) is sometimes organized in double seismic zones, usually showing down-dip compression and tension in the upper and lower parts of the slabs (Hasegawa et al., 1978), although significant exceptions occur (e.g., Nazca plate, Rietbrock and Waldhauser, 2004). This observation has been interpretad as related to slab unbending (Engdahl and Scholz, 1977; Kawakatsu, 1986).
Whatever the exact physical mechanism (Green and Zhou, 1996; Silver et al., 1995) that controls deep seismicity (focal depths > 300 km; Isacks and Molnar, 1971) slab tortions should be over and seismicity should be controlled by subduction driving mechanisms. The majority of moment release occurs in earthquakes with mechanisms associated with downdip compression (Isacks and Molnar, 1971; Bilek et al., 2005). Deep earthquakes are interpreted to occur in regions of high pull fraction (Bilek et al., 2005). Down-dip compression is typical in deep earthquakes in all Wadati-Benioff zones that reach the 670 km transition, and has been interpreted to reflect increasing resistance encountered by the subducting lithosphere (Isacks and Molnar, 1969 and 1971).
Although the pattern of stress in subducting slabs is highly complicated, the data of Isacks and Molnar (1971) indicate, for intermediate seismicity, a preference for down-dip tension in east-directed subduction zones (e.g., the Nazca plate in the Chile subduction zone, Rietbrock and Waldhauser, 2004, and the Cocos plate in the Mexican subduction zone, Manea et al., 2006) and down-dip compression in west-directed

subductions (e.g., Tonga, Chen and Brudzinski, 2001; Chen et al., 2004). This polarity-related pattern of the stress in slabs cannot be simply explained with the different age of subducting plates. In the central Mediterranean area, the Ionian lithosphere (probably oceanic and Mesozoic in age; Catalano et al., 2001) subducts westward under the Calabrian arc and eastward under the Hellenic arc. The Ionian lithosphere is part of the African plate and moves westard with respect of the mantle in all the hotspots reference frames. As shown in Fig. 1, the Hellenic east-directed slab is characterized by down-dip extension (Papazachos et al., 2005) whereas the Ionian (or Apennines) W-directed slab by compression (Frepoli et al., 1996).

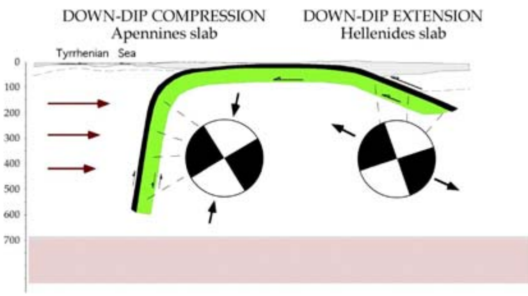

Figure 1. State of stress in the Ionian subduction plate beneath the Calabrian and Hellenic arcs (after Doglioni et al., 2007).

3. **Plate kinematics**

Hotspots provide a reference frame for absolute motion of plates (e.g., Norton, 2000). Hotspot tracks clearly indicate a relative motion between lithosphere and the underlying mantle, the asthenosphere acting as a detachment layer due to its low viscosity. Several researchers proposed a global or net westward drift of the lithosphere relative to the mantle (e.g., Bostrom, 1971; Ricard et al., 1991; Gripp and Gordon, 2002; Cuffaro and Jurdy, 2006), with average rates between 4.9 cm/yr (Gripp and Gordon, 2002) and 13.4 cm/yr (Crespi et al., 2007). If a shallow origin is assumed for hot spots, all the plates move westward with respect to the underlying mantle (Fig. 2) that, consequently, moves eastward with respet to the lithosphere (e.g., Cuffaro and Doglioni 2007). It is clear that, owing to the dip direction of the slabs with respect to the absolute plate motion, subductions may either oppose or accompany the relative mantle flow, in case slabs dip westward or eastward respectively. Typical subductions dipping to the west and east occur in the Marianas and in Chile (in the following the terms Marianas-like and Chile-like will be used to indicate alternatively dipping subduction zones).

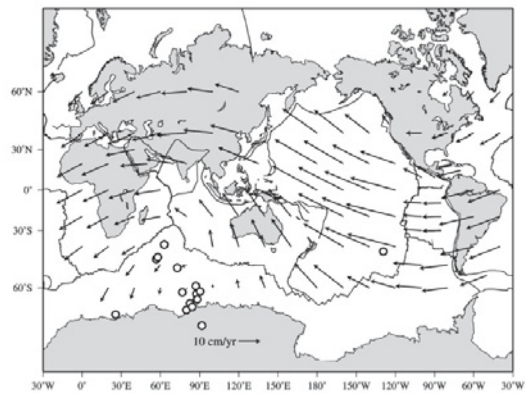

Figure 2. Plate velocities according to the deep hot spots reference frame (after Cuffaro and Doglioni, 2007).

4. **Use of COMSOL Multiphysics**

We model 2D sections in a plane strain approximation that include crust, lithospheric mantle (LID), upper mantle and lower mantle (Fig. 1), each layer being characterised by different rheological parameters. In order to avoid boundary effects, the model has a lateral extension much larger than the region we are interested in (i.e., the subductiong slab and the adjacent areas).

The model is characterised by a Maxwell linear viscoelastic rheology, which is considered to be appropriate to catch the global response of the system in the 250 kyr period that we consider.

Our plane strain dynamic modelling solves the compatibility equations

$$\varepsilon = \begin{Bmatrix} \varepsilon_x \\ \varepsilon_y \\ \varepsilon_{xy} \end{Bmatrix} = \begin{Bmatrix} \dfrac{\partial u}{\partial x} \\ \dfrac{\partial v}{\partial y} \\ \dfrac{\partial u}{\partial x} + \dfrac{\partial v}{\partial y} \end{Bmatrix} = \begin{bmatrix} \dfrac{\partial}{\partial x} & 0 \\ 0 & \dfrac{\partial}{\partial y} \\ \dfrac{\partial}{\partial y} & \dfrac{\partial}{\partial x} \end{bmatrix} \begin{Bmatrix} u \\ v \end{Bmatrix}.$$

the equilibrium equations for contiuous media

$$\frac{\partial \sigma_{ij}}{\partial x_i} + \rho X_i = \frac{\partial \sigma_{ji}}{\partial x_i} + \rho X_i = 0.$$

and the constitutive equations for Maxwell bodies

$$\dot{\varepsilon} = \frac{\dot{\sigma}}{2\mu_M} + \frac{\sigma}{2\eta_M}$$

The contact between the slab and the overriding mantle and between the lithosphere and the upper mantle is simulated *via* low viscosity layers (orange in Fig. 1) that act as detachment surfaces. The results give a dynamic snapshot of the response of the system to loads applied, neglecting processes (e.g., thermal) acting on longer timescales. Table I shows the viscous and elastic parameters adopted in the calculations for the various layers.

Table I: Elastic and viscous parameters adopted in the calculations

Layer	Young modulus (Pa)	Viscosity (Pa . s)	Poisson's ratio
Crust	$6x10^{10}$	$1x10^{24}$	0,25
Lithospheric mantle	$1.75x10^{11}$	$5x10^{22}$	0.27
Low viscosity layer	$1.27x10^{11}$	$5x10^{17}$	0.27
Upper mantle	$1.75x10^{11}$	$1x10^{21}$	0.27
Lower mantle	$1.27x10^{11}$	$1x10^{22}$	0.27

The isostatic forces need to be included in the model since they influence the tectonics-induced signal. Gravity is not applied as a body force through the model but is considered as an additional boundary condition (Winkler foundation; e.g., Williams and Richardson, 1991) at the surface, in terms of a vertical pressure ($-\Delta\rho g u$, where $\Delta\rho$ is the difference in density between crust and air at the surface, g is the gravity acceleration and u is the vertical displacement) opposing the surface displacement. This representation of the isostatic forces allow us to introduce easily density variations in the model according to the backstripping approximation (Bott, et al., 1989). The slab density anomalies are modelled in terms of differences with respect to a reference density profile in regions unaffected by the subduction process, to which a zero density is applied. In this way it is possible to include gravitational effects of density anomalies without applying real densities (which would result in a collapse of the modelled geometry) to the entire model. In particular a density anomaly of 60 kg/m^3 is applied, in the models where slab pull is active, in the region shown in Fig. 3.

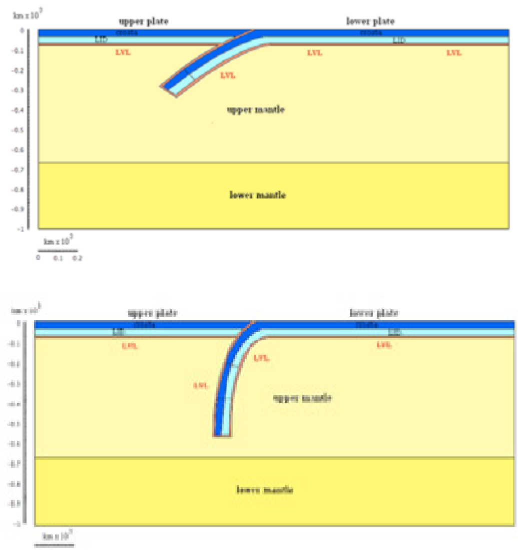

Figure 3. Geometry and materials of Chile- and Marianas-like models.

The density anomalies and the boundary conditions are activated instantaneously and kept constant for 250 kyr, until a dynamic equilibrium is reached between the tectonic and isostatic forces. The final configuration is considered to be an adequate representation of the stress field associated with the modelled geodynamic setting. Additional mechanical boundary conditions are the following: the bottom of the model is fixed in the vertical direction; the left and right lateral boundaries of the lithospere are kept fixed in the horizontal direction (but in some models, a 5 cm/a convergence between the two plates was simulated); the left and right boundaries of the mantle are either left free (when no mantle wind is simulated) or

alternatively a horizontal velocity (either right directed on the left boundary of left directed on the right bounday) of 8 cm/yr are applied in order to simulate the effects of mantle wind.
Cruciani et al. (2005) and Riguzzi et al. (2009) have shown that steep and shallow slabs are typical of subductions contrasting (normally west-dipping) and favoured by (normally east-dipping) relative mantle motion respectively. For this reason, we use different geometries (i.e., steep and flat subducting slabs; Fig. 3) for Marianas-like and Chile-like subduction zones. Only the results of a small part of these models will be shown and discussed in the following.

4. Modelling Results

Figure 4 and 5 show the distribution of the Von Mises stress in the region of the subducting slab for both Chile- and Marianas-like subduction zones. The Von Mises stress distribution has been calculated adopting various kinematics for both geometries. The Von Mises stress is function of the shear stress and as such gives an indication of the areas in which earthquakes are expected to occur (i.e., areas of high shear stress and consequently of high Von Mises stress). Both figures show a stress concentration at the slab bend and at the tip of the slab. Areas of maximum curvatures of subducting slabs are characterised, in nature, by concentration of strong earthquakes, consistently with modelling results.
Figures 6 and 7 show that the state of stress of subducting slabs is controlled by the density anomalies and by the kinematics of the subduction system. The six panels show, for each geometry (Chile- and Marianas-like), the principal stress axes predicted by three models in which subduction is forced: 1) only by negative buoyancy associated with the density contrast (slab pull); 2) by slab pull and mantle flow in a direction (from left to right) opposite to the dip of the slab; 3) by slab pull and mantle flow in the same direction (from right to left) of the dip of the slab. It is evident that slabs encroached by the mantle wind with a direction opposite to that of dip of the slab (e.g., east-directed motion of the mantle and west-dipping slab and vice versa) are characterised by stress states showing along-dip

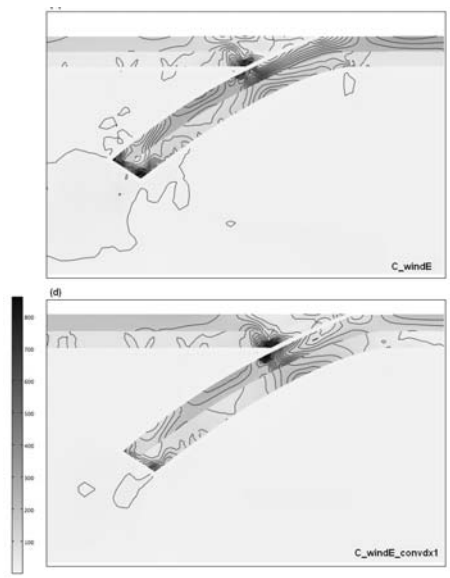

Figure 4. Von Mises stresses (in MPa) calculated for models with Chile-like geometries and characterised by mantle flow in the same direction of subduction (top) and by mantle flow and convergence (bottom).

Figure 5. Von Mises stresses (in MPa) calculated for models with Marianas-like geometries and characterised by mantle flow opposite to the direction of subduction (top) and by mantle flow and convergence (bottom).

compression. Slabs sustained by the mantle wind (e.g., east-directed motion of the mantle and east-dipping slab or west directed motion of the mantle and west-dipping slab or west directed) are characterised by along-depth tensional state of stress.

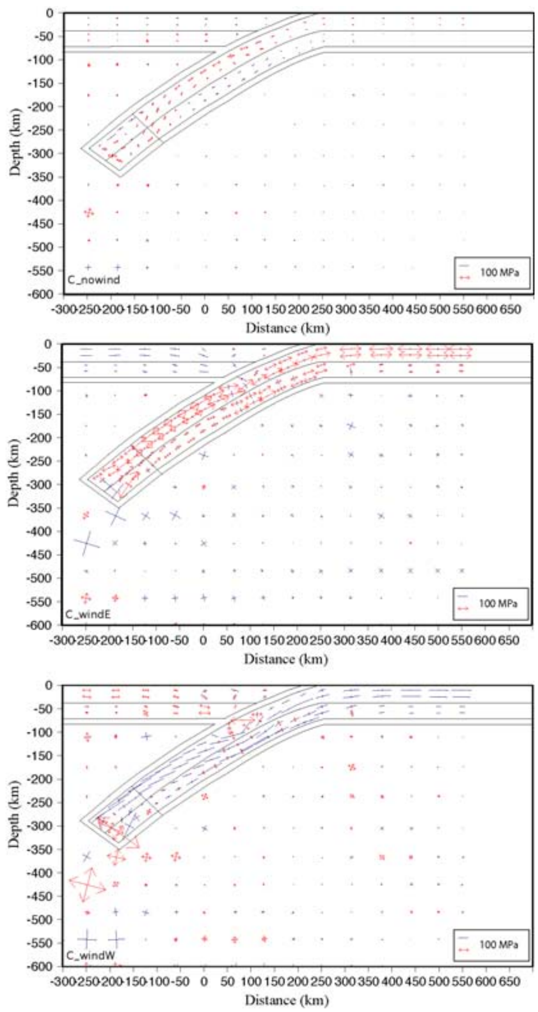

Figure 6. Principal stress axes for models characterised by (top) slab pull, (centre) right directed mantle wind and (bottom) left directed mantle wind. Blue lines indicate compressional and red lines tensional stresses. Model results are for Chile-like subductions.

5. Conclusions

Two dimensional plane strain viscoelastic models of subduction zones were performed in order to calculate the state of stress within subducting slabs and compare it with available geophysical observations.

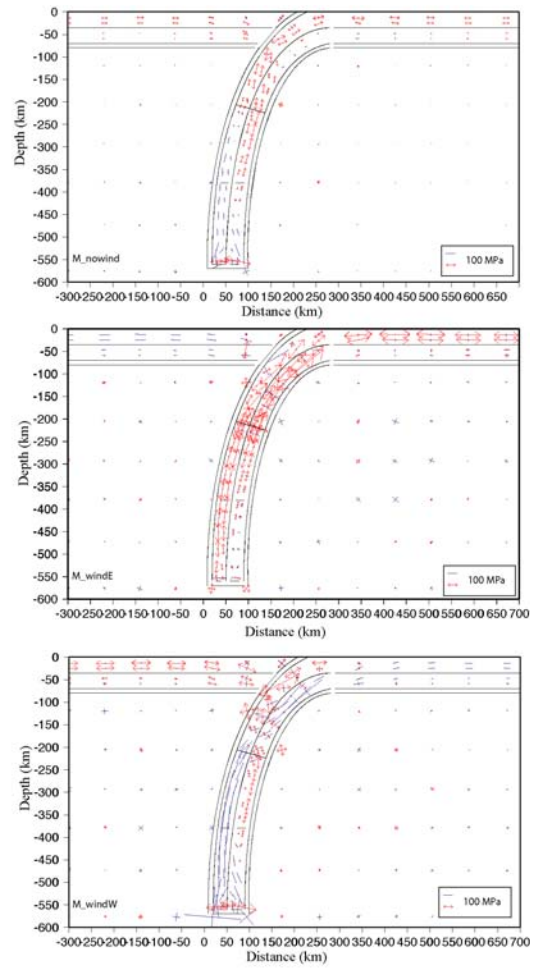

Figure 7. Principal stress axes for models characterised by (top) slab pull, (centre) right directed mantle wind and (bottom) left directed mantle wind. Blue lines indicate compressional and red lines tensional stresses. Model results are for marianas-like subductions.

The following conclusions were drawn:

1) The concentration of Von Mises stress is controlled by the geometry (curvature) of the slab; maximum concentration of stress occurs at the hinge of subducting slabs, consistently with observations.

2) Absolute plate kinematics is fundamental for the definition of the state of stress of subducting slabs; downdip compression in subducting slab is enhanced by mantle flow opposing the dip of the

slab, whereas overall downdip extension is favoured by mantle flow in the same direction of the slab dip.

6. References

Bilek, S.L., Conrad, C.P. and Lithgow-Bertelloni, C., Slab pull, slab weakening, and their relation to deep intra-slab seismicity. *Geophys. Res. Lett.*, **32** ,doi:10.1029/2005GL022922 (2005)

Bostrom, R. C., Westward Displacement of the Lithosphere. *Nature* **234**, 536 - 538; doi:10.1038/234536a0 (1971).

Catalano, R., Doglioni, C., Merlini, S., On the Mesozoic Ionian basin. *Geophys. J. Int.*, **144**, 49-64 (2001).

Bott, M. H. P., Waghorn, G. D. and Whittaker, A., Plate boundary forces at subduction zones and trench-arc compression. *Tectonophysics*, **170**, 1-15 (1989).

Chen, W.P. & Brudzinski, M.R., Evidence for a large-scale remnant of subducted lithosphere beneath Fijii. *Science,* **292**, 2475-2479 (2001).

Chen, P.-F., et al., A global survey of stress orientations in subducting slabs as revealed by intermediate depth earthquakes, *Geophys. J. Int*., **159**, 721– 733 (2004).

Crespi, M., Cuffaro, M., Doglioni, C., Giannone, F., Riguzzi, F., Space geodesy validation of the global lithospheric flow. *Geophys. J. Int.,* **168**, 491–506 (2007).

Cruciani, C., Carminati, E., Doglioni, C., Slab dip vs. lithosphere age: No direct function. *Earth and Planetary Science Letters* ***238***, 298-310 (2005).

Cuffaro, M., and Doglioni, C., Global kinematics in deep versus shallow hotspot reference frames, in Foulger, G.R., and Jurdy, D.M., eds., Plates, plumes, and planetary processes: *Geological Society of America Special Paper,* **430**, 59-374, doi: 10.1130/2007.2430(18) (2007).

Cuffaro, M., Jurdy, D.M., Microplate motions in the hotspot reference frame. *Terra Nova,* **18**, 276–281 (2006).

Doglioni, C., Carminati, E., Cuffaro, M. and Scrocca, D., Subduction kinematics and dynamic constraints. *Earth Science Reviews*, **83**, 125-175 (2007).

Engdahl, E.R., Scholz, C.H., A double Benioff zone beneath the central Aleutians: An unbending of the lithosphere. *Geophys. Res. Lett.*, **4**, 473–476 (1977).

Frepoli, A., Selvaggi, G., Chiarabba, C., Amato, A., State of stress in the Southern Tyrrhenian subduction zone from fault-plane solutions. *Geophys. J. Int*. **125**, 879–891 (1996).

Green, H. W. and Zhou, Y., Transformation-induced faulting requires an exothermic reaction and explains the cessation of earthquakes at the base of the mantle transition zone. *Tectonophysics*, **256**, 1-4, 39-56 (1996).

Gripp, A.E., Gordon, R.G., Young tracks of hot spots and current plate velocities. *Geophys. J. Int*. **150**, 321-361 (2002).

Hasegawa, A., Umino, N., Takagi, A., Double-planed structure of the deep seismic zone in the northeastern Japan arc. *Tectonophysics* **47**, 43–58 (1978).

Isacks, B. & Molnar, P., Distribution of stresses in the descending lithosphere from a global survey of focal mechanism solutions of mantle earthquakes, *Rev. Geophys. Space Phys*. **9**, 103-174 (1971).

Isacks, B., Molnar, P., Mantle Earthquake Mechanisms and the Sinking of the Lithosphere. *Nature* **233**, 1121 (1969).

Kawakatsu, H., Double seismic zones: kinematics. *J. Geophys. Res*. **91**, 4811–4825 (1986).

Manea, V., Manea, M., Kostoglodov, V., Sewell, G., Intraslab seismicity and thermal stress in the subducted Cocos plate beneath central Mexico. *Tectonophysics* **420**, 389-408 (2006).

Norton, I.O., Global hotspot reference frames and plate motion.In: Richards, M.A., Gordon, R.G., Van der Hilst, R.D. (Eds.), The History and Dynamics of Global Plate Motions. *Geophysical Monograph,* **121**, 339–357 (2000).

Papazachos, B.C., Dimitriadis, S.T., Panagiotopoulos, D.G., Papazachos, C.B., Papadimitriou, E.E., Deep structure and active tectonics of the southern Aegean volcanic arc. In: Fytikas, M., Vougioukalakis, G.E. (Eds.), The South Aegean Active Volcanic Arc. *Developments in Volcanology*, **7**, 47–64 (2005).

Ricard, Y., Doglioni, C. and Sabadini, R., Differential rotation between lithosphere and mantle: a consequence of lateral mantle viscosity variations. *J. Geophys. Res.*, **96**, 8407-8415 (1991).

Rietbrock, A. and Waldhauser, F., A narrowly spaced dounle-seismic zone in the subducting Nazca plate. *Geophysical research letters*, Vol.**31**, L10608, doi:10.1029/2004GL019610 (2004).

Riguzzi, F., Panza, G., Varga, P. and Doglioni, C., Can Earth's rotation and tidal despinning drive plate tectonics? *Tectonophysics*, doi:10.1016/j.tecto.2009.06.012 (2009).

Seno, T., Yamanaka, Y., Double seismic zones, deep compressional trench—outer rise events and superplumes. In: Bebout, G.E., Scholl, D.W., Kirby, S.H., Platt, J.P. (Eds.). Subduction Top to Bottom, vol. 96. AGU, Washington, DC, *Geophys. Monogr.*, **347**–355 (1996).

Silver, P. G., Beck, S. L., Wallace, T. C., Meade, C., Myers, S. C., James, D. E. and Kuehnel, R., Rupture Characteristics of the Deep Bolivian Earthquake of 9 June 1994 and the Mechanism of Deep-Focus Earthquakes. *Science*, Vol. **268**. no. 5207, pp. 69 – 73 (1995).

Williams, C.A., Richardson, R.M., A rheological layered three-dimensional model of the San Andreas Fault in central and southern California. *J. Geophys. Res*. **96**, 16597 – 16623 (1991).

9. Acknowledgements

Research supported by Sapienza (Ateneo) and MIUR fundings Carlo Doglioni is thanked for stimulating discussions. Maurizio Battaglia is thanked for providing access to COMSOL.